

# CMP9135M Applying Computer Vision techniques for feature extraction and texture analysis on skin Lesions



## UNIVERSITY OF LINCOLN

line 1: 2<sup>nd</sup> Stephen Rerri-  
Bekibele  
line 2: *School of Computer  
Science. University of Lincoln  
(of Affiliation)*  
line 3: Lincoln, United Kingdom  
line 4:  
16663359@students.lincoln.ac.  
uk

### Table of Contents

Introduction.....	2
A. TASK 1 Image Segmentation and Detection 2	
B. Task 2 Feature Calculation.....	2
C. Task 3 Object Tracking.	3
Task 1 images .....	4
Task 2 images .....	5
Task 3 images .....	7
Task 3 with Validation Gating enabled.....	7

**Abstract—** The accurate and clear detection of diseases or abnormalities is very necessary and relevant in modern problems ranging from Medical to vehicle automation. This report tackles the problems of Image segmentation, Feature Calculation and Object tracking in 3 different scenarios. 1. The detection and segmentation of skin lesions. 2. Feature calculation of a given image. 3. Object tracking and plotting of a moving target according to a generic frame to frame image segmentation of a target.

**Keywords—**Feature Calculation, Medical, skin lesions, image segmentation, object tracking, detection (key words)

## INTRODUCTION

### A. TASK 1 Image Segmentation and Detection

To segment lesions from images a few steps have to be taken.

Two methods were devised to increase the effectiveness of the object segmentation. If a sample had a higher score in either method that score was taken instead. This meant that where one method failed to get an accurate segmentation of an object, the other got a significantly better segmentation. The methods largely had the same steps but differed in a few key places.

Both methods were created in a function called compute dice score which took in each image and enhanced them by mapping the intensity values to a new output variable by saturating the top 1% and bottom 1% of all the pixel values effectively increasing the contrast of the output image.

In method 1 K-means clustering was then used to separate the image into three different clusters, this partially segmented the lesions from the skin after which the erode function was used with a flat structuring element of shape ball to remove some of the unnecessary spots from the image. At this stage the image was finally converted to grey and binarized. The edges of the image were then detected and specks touching the borders of the image were removed before any remaining small blobs were erased. The remaining hole was filled in and the resulting image could then be compared against the ground truth.

The method 2 method used the same method as the first but skipped the k-means classification step and instead went on to converting the image to grayscale after enhancing it. In this method the grey images were then inverted because the grayscale image when binarized already had a clear outline of the lesion. This

inversion made the holes the lesion instead of the background and vice versa.

In the same way as above, any specks that were touching the image boarder were now removed, blobs were removed and the newly created “lesion holes” from inverting the image were filled in.

Testing showed that doing these actions in this order helped to make images that had poor lesion detection at the end of the method 1, come out much better in method 2 and result in a better lesion detection. The addition of method 2 raised the lesion detection accuracy from 59% to 80%.

### B. Task 2 Feature Calculation

For this task the frequency domain of the image was calculated and displayed at different angles to see how the angles and directions affected the resulting image.

The resulting Fourier domain showed each point representing a particular frequency contained in the spatial domain image. To analyse the textures in the image the frequency domain had to be observed.

The image was converted to the Fourier domain in order to find the spectral features. To calculate the feature for various radiuses the equation below was implemented:

$$S(r) = \sum_{\theta=0}^{\pi} S(r, \theta)$$
$$S(\theta) = \sum_{r=0}^{N/2} S(r, \theta)$$

The various radiuses used were plotted in a graph and the various angles from 0-360 were also plotted in a separate graph. To view the effect of changing the radius simply pick a choice of radius in the radius\_values index by picking a value between 1 and 7.

To express the spatial domain in polar coordinates we get the new coordinates of the image by dividing the image in two and multiplying the radius by the sin of each angle for the height of the image and radius by cos each angle for the width of the image and then compute the Fourier transform of the polar coordinates for S\_r\_theta.

With the Fourier transform we can now calculate S\_r values for each radius and S\_theta for each angles. S\_r is calculated as the sum of all the pixels in the Fourier transform at the given radius. S\_theta is calculated as the sum of all the pixels Fourier transform at angle theta. Results showed that as the radius increased, the

number of features decreased therefore the number of features is inversely proportional to the size of the radius.

This means there is a negative correlation between the radius size and number of features.

To select features for calculation from the co-occurrence matrix and grey level run length matrix two functions were written.

For the gray co-occurrence matrix the image was first converted to grayscale and then a histogram is calculated for all the gray levels of the image. From the histogram the statistics such as mean, variance, skewness, kurtosis, energy and lastly entropy are all calculated.

The results showed that the mean value for the probability density of occurrence of the intensity of the image was  $\sim 4$ .

To extract the texture features the Gray Level Run Length matrix was implemented by converting the image to grayscale, providing a quantize value and a binary mask of the image to use with values of 1 at the region of interest.

Next the range of the image was calculated by retrieving the min and max pixel values of the image and then the image was quantized to discrete integer values between 1 and the set quantize value. Four different degree angles, 0, 45, 90 and 135 were then tested and the pixels for each quantization level were recorded.

To finish off, the features for the four angles were calculated. The results showed that in all cases only GLN, RLN and HGRE were read.

With a quantization level of 4 RLN was the lowest value and GLN and HGRE were joint first. When a quantization level of 6 was tested, all 3 values increased but RLN was still the lowest and HGRE and GLN were joint first yet again. Lastly, when a quantization level of 8 was chosen however, RLN was the highest value with GLN and HGRE coming in joint second.

### *C. Task 3 Object Tracking*

Task 3 involved displaying the trajectory of a tracked image according to its pixel positions. Two graphs were plotted and compared. One was the real coordinates of the moving target and the second was the estimated trajectory from a noisy equivalent provided by a generic video detector. The mean, standard deviation of the absolute mean error and the root mean squared error were calculated.

With Validation Gating the Plot of the predicted trajectory was significantly different. Without validation gating the

root mean square error was 3.0602 and with Validation gating the root mean squared error was 81.9306.

TASK 1 IMAGES

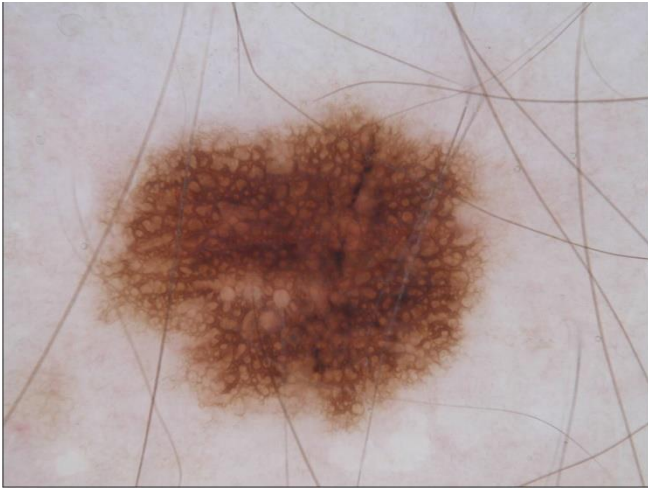


Figure 1. ISIC\_19 DICE\_SCORE 0.8678

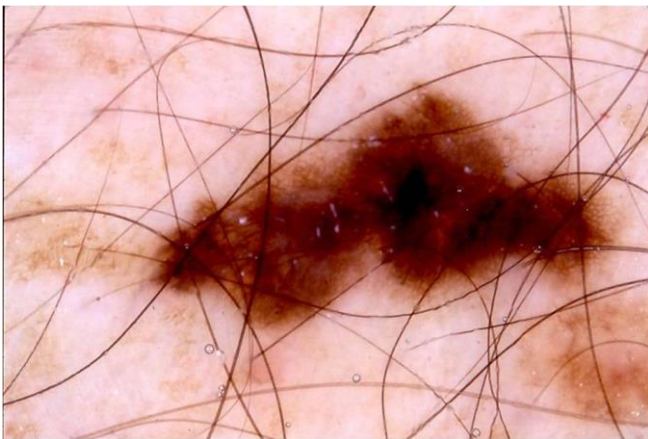
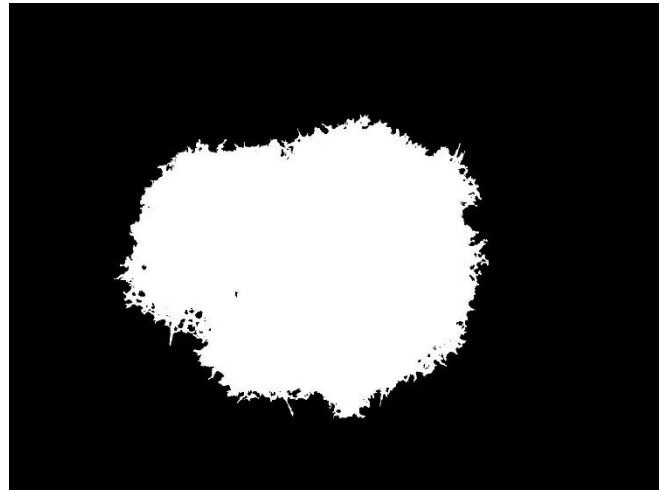


Figure 2. ISIC\_214 DICE\_SCORE 0.8525



Figure 3. ISIC\_95 DICE\_SCORE 0 (number 33)



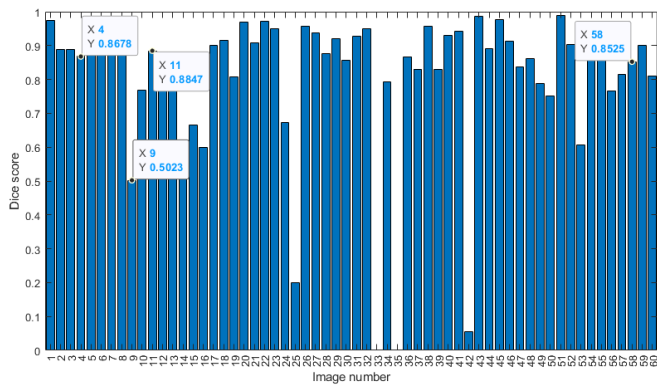


Figure 4. Graph of images and dice score

### TASK 2 IMAGES

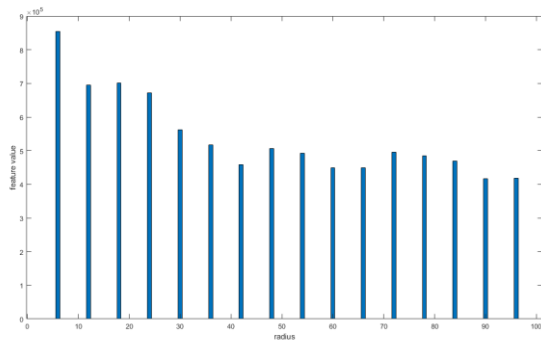


Figure 5. radius 100 radius graph

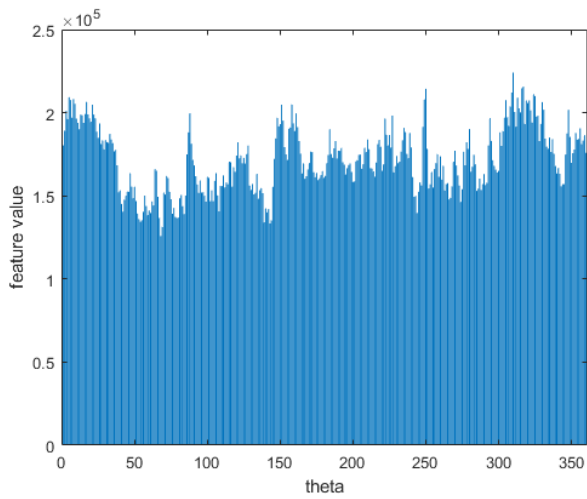


Figure 6. Radius 100 theta graph

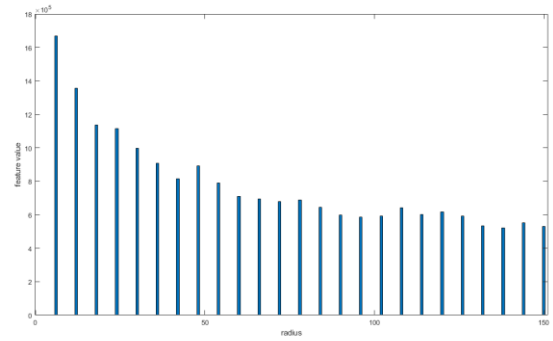


Figure 7. Radius 100 theta graph

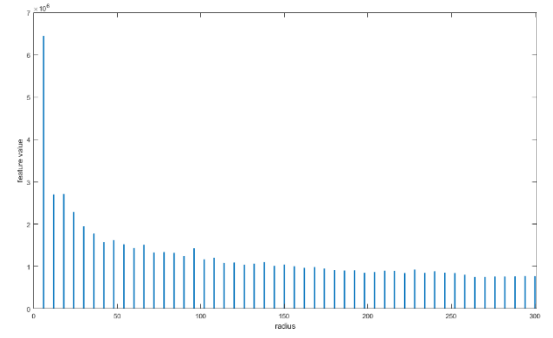


Figure 8. Radius 200 radius graph

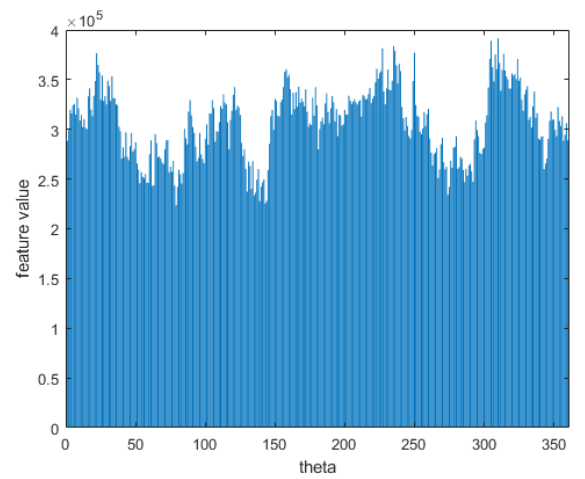


Figure 9. Radius 200 theta graph

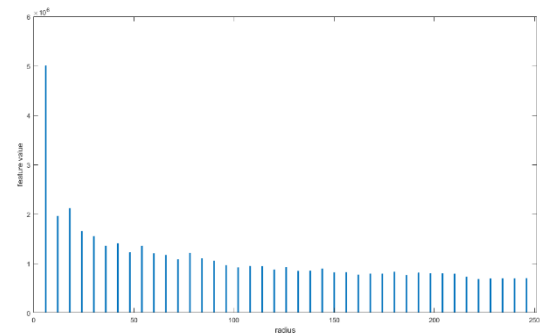


Figure 10. radius 250 radius graph

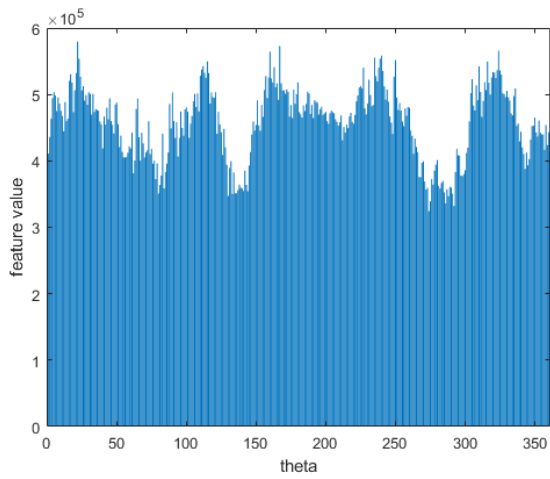


Figure 11. Radius 250 theta graph

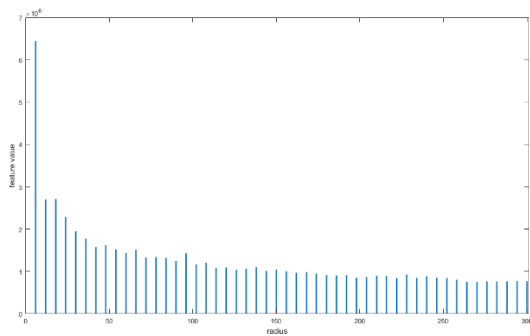


Figure 12. Radius 300 radius graph

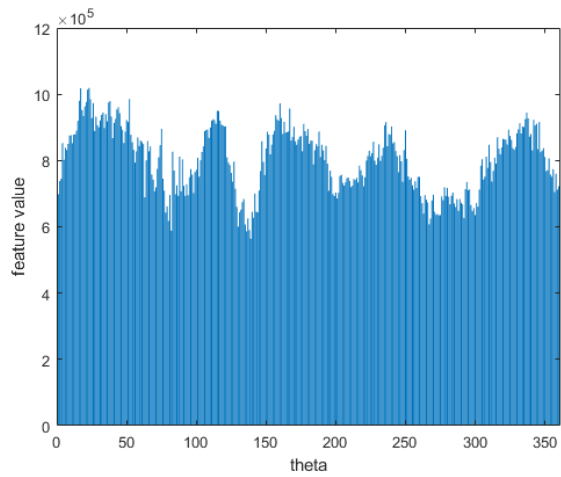


Figure 13. radius 300 theta graph

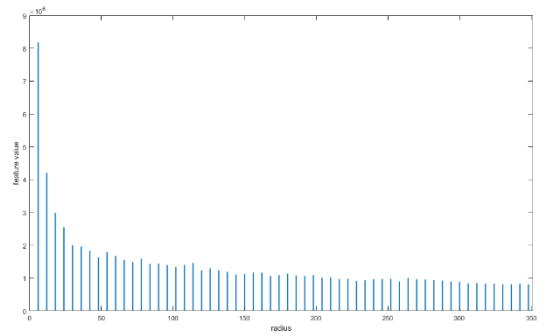


Figure 14. radius 350 radius graph

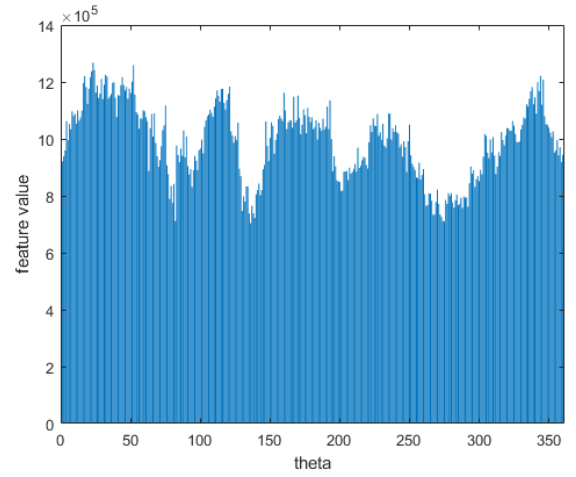


Figure 15. Radius 350 theta graph

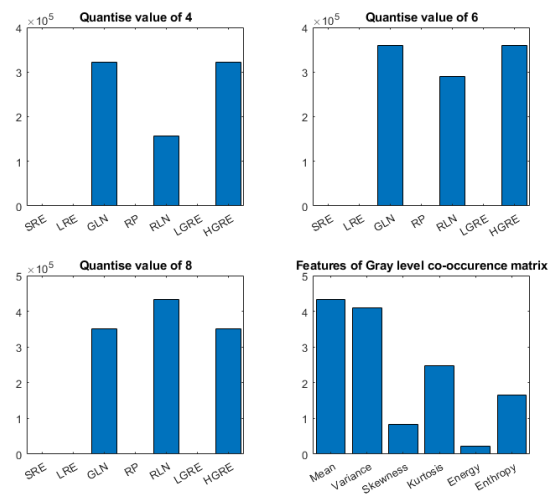
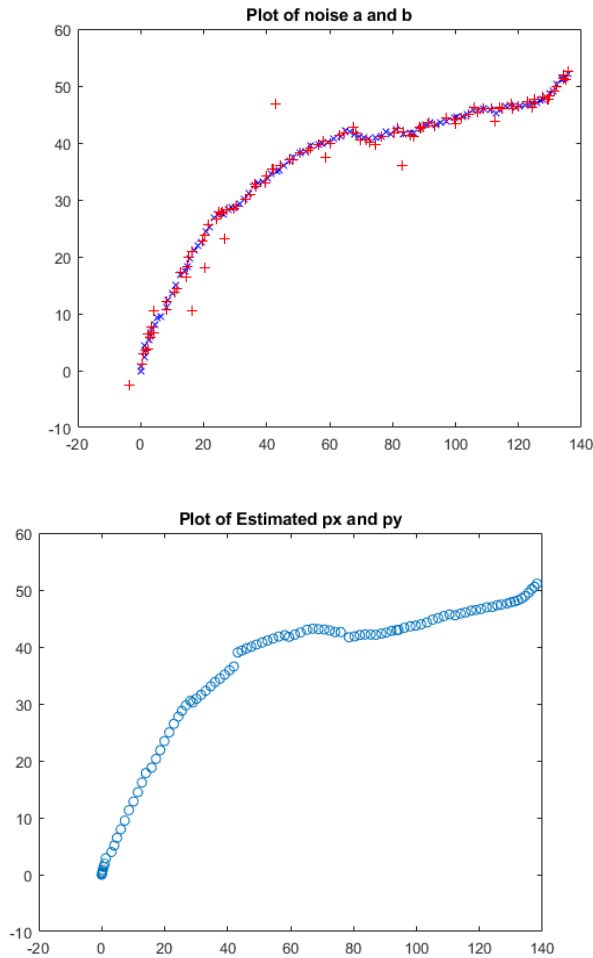
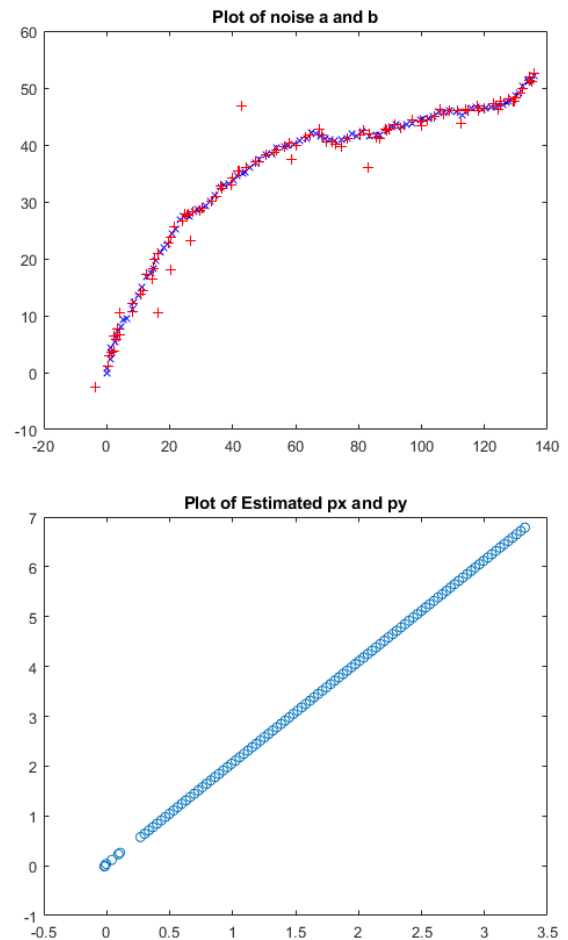


Figure 16. Gray level run length matrix and gray co-occurrence matrix plots

### TASK 3 IMAGES



### TASK 3 WITH VALIDATION GATING ENABLED



### ACKNOWLEDGMENT

I would like to the computer Vision Lecturers for their useful workshop sessions and Lecturers that brought the wonders of computer vision to my attention

### REFERENCES

- [1] Computer vision Lecture and workshop 2, Image segmentation, available at: <https://uol.cloud.panopto.eu/Panopto/Pages/Viewer.aspx?id=ee233d9e-9e2f-43d1-b2df-ae4d00c6b485> [accessed 18/05/2022]
- [2] Computer vision Lecture and Workshop 3, Morphological Operation and Image Segmentation. Available at: <https://uol.cloud.panopto.eu/Panopto/Pages/Viewer.aspx?id=15b5a3d3-285e-4e76-9a97-ae5400c6f25f>
- [3] Computer Vision workshop 5 , Fourier Analysis and Co-Occurrence Matrix, available at: <https://uol.cloud.panopto.eu/Panopto/Pages/Viewer.aspx?id=a7979472-fdf0-4912-9307-ae6200ca6fff>
- [4] Computer Vision workshop 8 Kalman Filter for Visual Tracking. Available at: <https://uol.cloud.panopto.eu/Panopto/Pages/Viewer.aspx?id=5300f390-b76b-4306-a337-ae8500b5eeec>